Chaos, Solitons and Fractals 131 (2020) 109490

Contents lists available at ScienceDirect

Chaos, Solitons and Fractals

Nonlinear Science, and Nonequilibrium and Complex Phenomena

journal homepage: www.elsevier.com/locate/chaos

One-dimensional reaction-diffusion dynamics in spatially bounded domains

Francesco Sarnari [a,b]

[a] University of Pisa, Physics Department, Italian National Research Council (CNR), Italy
[b] Biophysics Institute, University of Siena School of Information Engineering and Mathematical Sciences, Italy

ARTICLE INFO

Article history:
Received 27 May 2019
Revised 8 October 2019
Accepted 11 October 2019
Available online 24 December 2019

ABSTRACT

We consider the complex dynamics arising in a one-dimensional advection-reaction-diffusion system along with its bistable cubic variant. In both cases, we analyze the dynamics in a bounded domain, assuming, first, Robin, and then periodic boundaries. We study the stability of the solutions obtained and suggest eventual implications in the experimental study of chemical waves as well as in a simplified description of cardiac electric signal propagation.

1. Introduction

Reaction-diffusion systems play a significant role in modelling chemical and biological systems, in which a variety of pattern formations has been observed [1–8].

Therefore, the mechanisms which drive pattern formation in reaction-diffusion systems are worth investigating because of their sheer breadth of applicability, from Chemistry to Biology to Physiology and beyond [9–19].

Reaction-diffusion systems often possess symmetries [20,21]. Specifically, the equations describing reaction-diffusion systems are often left unchanged by certain groups of transformations, such as Euclidean symmetries. In that framework, symmetry-breaking refers to a situation in which the solutions to the equations have less symmetry than the equations themselves. Therefore, symmetry-breaking is extremely important in the investigation of reaction-diffusion patterns, since the solutions often arise via symmetry-breaking bifurcations, and the behaviour of solutions is strongly dictated by the nature of the symmetry-breaking. The simplest PDE describing a reaction-diffusion system was studied by Kolmogorov et al. in 1937 [22], namely the FKPP (Fisher, Kolmogorov, Piskunov, Petrovskii) equation, in relation to a problem of population dynamics. The reaction in that case is described by a logistic growth term, with stationary states corresponding to 0 and 1, the former unstable, the latter stable. A small perturbation of the unstable state produces travelling wave fronts propagating towards the stable state.

The goal of the present work is to look at the dynamics arising in a single-species reaction-diffusion system characterized by the presence of a throughflow within a bounded domain, with the system being driven outside of equilibrium.

Most of the work on reaction-diffusion systems has investigated dynamics on the infinite line of fronts connecting homogeneous steady states [23–26]. For example, Taylor et al. [27] consider in their experimental setting the dynamics generated by the propagation of chemical waves in a tubular packed-bed reactor where the radius of the tube is much smaller than its length, thus making the one-dimensional approximation appropriate. These dynamics are well described by the FKPP equation with advection, along with its cubic variant in case of bistability.

The main novelty of our approach consists in the analysis of the dynamics produced by these equations in a spatially bounded domain. More specifically, we examine the existence and eventual stability of travelling waves.

Advection-reaction-diffusion (ARD) equations of this type turn out to be appropriate in modelling a variety of natural phenomena.

In the context of human physiology, ARD systems have extensive applicability in describing the complex dynamics arising in excitable media [28–34]. Despite the fact that most of these studies refer to bi-dimensional systems, we find particularly interesting the study of Beck et al. [35], who initially consider a Fitzhugh-Nagumo system [36–38], and then deduce that even a one-dimensional approximation would offer a suitable description of the cardiac action potential propagation.

The Beck model confines itself to the semi-infinite line, while we believe that our approach will allow a more realistic revisitation of their work by looking at the resulting dynamics in a bounded domain.

We believe that such an analysis will be useful in understanding propagation of electrical activity in the cardiac muscle [39]. In

E-mail address: sarnari@diism.unisi.it

https://doi.org/10.1016/j.chaos.2019.109490
0960-0779/

fact, the inceptive phase of cardiac activity takes place in the sinoatrial (SA) node, formed by a small nucleus of cells with the ability to excite themselves autonomously, thus initiating the heartbeat, with the electric signal propagating towards the atrioventricular (AV) node. This phenomenon could be described by a lumped one-dimensional model, which resembles the model equations investigated in this paper.

In our study two sets of boundary conditions are considered in a finite box: first Robin, and then periodic. Robin boundary conditions [40] can be useful in describing the propagation of the electric signal from the SA to the AV node, which leads to heart muscle contraction. By contrast, periodic boundary conditions can play a significant role in modelling the stability of reentrant spiral waves, by investigating their stability properties in a one-dimensional annular domain.

The dynamics arising in reaction-diffusion systems with Robin boundary conditions (in other settings called albedo boundary conditions) have already been investigated in the past. In particular, Hassan et al. [41] looked at a 1D analytically solvable Ballast resistor, while Wio et al. [42] studied a 2D activator-inhibitor model. In contrast with our equation, neither of these models considers the presence of advection, but rather explain in detail the effects produced on the solutions, from full absorption, to partial reflection, to full reflection at the boundaries as albedo parameters are varied.

Still in the context of 2D systems, it is worth mentioning the works of Rovinsky et al. [43] as well as Ponce Dawson et al. [44], whose efforts focused on the effects produced by advection in the Turing system [45]. The former shows the relevance of a throughflow in destabilizing the homogeneous steady pattern into a travelling-wave pattern, while the latter demonstrates the additional effect produced by anisotropic diffusion, where Turing instability, advection and anisotropic diffusion can produce a spatial pattern or even compete with each other, leading to the suppression of the pattern.

In our study both these approaches are combined, and, in the simpler setting of a 1D system we investigate the effects produced by the absence, first, and then the presence, of translational symmetry, depending on different boundary conditions, in a system characterized by a reflection symmetry-breaking, due to the presence of a throughflow.

The work is structured as follows: initially we investigate the linear theory, that which provides the set of linear instabilities, discussing first steady and then oscillatory cases. Thereafter, our analysis focuses on the first nonlinear approximation, aiming to find, close enough to the primary instability, a simplified description in terms of an amplitude equation, obtained by taking into account only the slow modes. We perform this analysis, first with Robin boundaries, and then in an annular domain.

Next, in the nonlinear regime, for both quadratic and cubic nonlinearities, we discuss steady solutions and travelling waves, along with their stability. The last section summarizes the obtained results.

2. Materials and methods

Let us consider $L>0$ and define the open domain $D=\{(x,t)|x\in[-L,L],t\in[0,+\infty[\}$. We will investigate the dynamics of some solutions of the equation

$$\partial_t\Phi(x,t) = c\partial_x\Phi(x,t)+\varepsilon\partial_{xx}\Phi(x,t) + \mu\Phi(x,t)-\Phi^2(x,t), \qquad (x,t)\in\mathcal{D} \tag{1}$$

or its bistable cubic variant:

$$\partial_t\Phi(x,t) = c\partial_x\Phi(x,t)+\varepsilon\partial_{xx}\Phi(x,t) + \mu\Phi(x,t)-\Phi^3(x,t), \qquad (x,t)\in\mathcal{D} \tag{2}$$

where c is an advection velocity, ε a diffusion coefficient, μ_0 a forcing term, and Φ interpreted as the concentration of a chemical reactant in $(x,t)\in\mathcal{D}$.

We initially consider the case of Robin boundary conditions

$$\begin{cases}(1-\beta)\partial_x\Phi+\beta\Phi=0 \ \text{ at } \ x=L\\ (1-\gamma)\partial_x\Phi+\gamma\Phi=0 \ \text{ at } \ x=-L\end{cases}$$

which represents the most general form of insulating boundaries.

Our analysis combines analytical and numerical techniques. The analytical investigation is performed by perturbation theory and multiple scales, leading to a centre manifold reduction, where the fast modes can be ignored as compared to the slow ones.

As to the numerical study, the time-stepping PDE has been integrated using a semi-implicit Crank–Nicolson numerical scheme, which is unconditionally stable, while the steady-state ODEs have been treated as a boundary value problem and integrated by the shooting method.

Put simply, our goal is to investigate some solutions of our PDE when two different symmetries - reflection and translation - are broken.

Before proceeding to the results section, let us pause for a moment to look at the scaling properties of Eq. (1). If we set $\bar{x}=\frac{x}{L}$, we can rescale the length of our domain, and rewrite our PDE as

$$\partial_t\Phi=\frac{\varepsilon}{L^2}\partial_{\bar{x}\bar{x}}\Phi+\frac{c}{L}\partial_{\bar{x}}\Phi+\mu\Phi-\Phi^2.$$

Now, we can also set new measuring units for time t and solution Φ

$$T=\delta t \ \text{ and } \ \phi=\sigma\Phi$$

in such a way that our PDE becomes

$$\partial_T\phi=\frac{c}{\delta L}\partial_{\bar{x}}\phi+\frac{\varepsilon}{\delta L^2}\partial_{\bar{x}\bar{x}}\phi+\frac{\mu}{\delta}\phi-\frac{\sigma^{-1}}{\delta}\phi^2.$$

At this point, if we want the coefficient of the nonlinear term to be 1, we set $\sigma^{-1}=\delta$ and obtain

$$\partial_T\phi=\frac{c}{\delta L}\partial_x\phi+\frac{\varepsilon}{\delta L^2}\partial_{xx}\phi+\frac{\mu}{\delta}\phi-\phi^2.$$

Here we still can choose δ arbitrarily, and therefore we might choose $\delta=\varepsilon$, so that $\sigma=\frac{1}{\sqrt{\varepsilon}}$ and, by redefining $c'=\frac{c}{\varepsilon}$, $\varepsilon'=1$, and $\mu'=\frac{\mu}{\varepsilon}$ ($\mu_0'=\frac{\mu_0}{\varepsilon}$ and $\mu_0'=\frac{\mu_1}{\varepsilon}$), end up with

$$\partial_T\phi=\frac{c'}{L}\partial_x\phi+\frac{1}{L^2}\partial_{xx}\phi+\mu'\phi-\phi^2. \tag{3}$$

Similarly, we might have chosen $\delta=c$ or $\delta=\mu$, thus ridding ourselves of one parameter. This shows that with no loss of generality we are free to keep one parameter fixed and vary the others, i.e., there are only three independent parameters in this problem. We can therefore decide to set $\varepsilon=1$ throughout.

3. Results

The results presented in this section follow the logical order outlined by perturbation theory. Initially, we focus on linear theory and discuss the eventual occurrence of Hopf bifurcation. Thereafter, we move to consider the weakly nonlinear approximation, where, for both nonlinearities, the steady branches are identified along with their stability. Our next step, in both cases, discusses in detail the steady-state solutions. The second part of this section mirrors the first one, where Robin boundary conditions are replaced by periodic ones.

3.1. Robin boundary conditions

Let us begin, then, the analysis of our partial differential equation (PDE) by focusing on linear theory, which incorporates the whole set of instabilities and corresponding growth/decay rates.

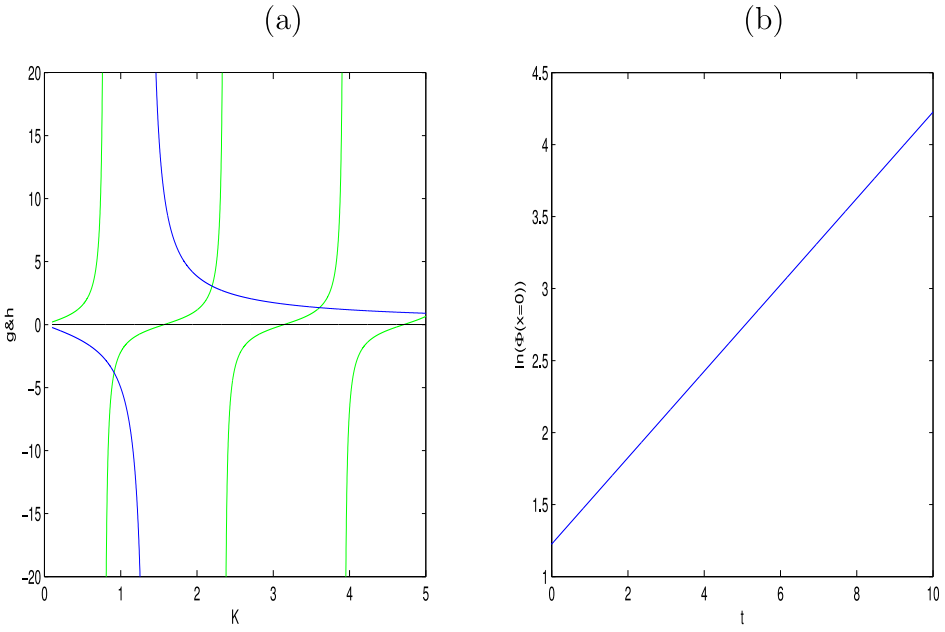

Fig. 1. (a) The dispersion relation. The labels g and h represent, respectively, left-hand (green) and right-hand (blue) sides of the dispersion relation. The plot corresponds to the selected parameters $c = 1,\ L = 2,\ \beta = 0.8,\ \gamma = 0.2$; (b) For $\mu > \mu_f$ the exponent p is positive and the solution of Eq. (5) grows. (For interpretation of the references to colour in this figure legend, the reader is referred to the web version of this article.)

3.1.1. Linear theory

We adopt a perturbation theory approach, and search for approximate solutions in the form of an expansion of Φ in powers of a small parameter δ

$$\Phi(x, T, t) = \delta A(T)\phi(x, t) \tag{4}$$

where $T = \delta t$ is the slow time, $\delta \ll 1$ is a dimensionless parameter, $\phi(x,\ t)$ is the linear eigenfunction, and where we have assumed that the PDE is separable.

Substituting (4) into Eq. (1), then at the leading order of δ we obtain the equation for the linear eigenfunction, which does not depend on amplitude A

$$\partial_t\phi = \frac{1}{L^2}\partial_{xx}\phi + \frac{c}{L}\partial_x\phi + \mu\phi. \tag{5}$$

The drift term is responsible for the break in the reflection symmetry ($x \to -x$) as well as for the presence of asymmetric boundary conditions (with $\gamma \neq \frac{\beta}{2\beta-1}$), while the presence of finite boundaries produces a break in the translational symmetry ($x \to x + L$). If we define the linear differential operator

$$\mathcal{L} := \frac{1}{L^2}\partial_{xx} + \frac{c}{L}\partial_x + \mu$$

our problem becomes

$$\partial_t\phi = \mathcal{L}\phi \tag{6}$$

subjected to boundary conditions

$$\begin{cases}(1-\beta)\partial_x\phi + \beta L\phi = 0 \ \text{ at } \ x = 1\\ (1-\gamma)\partial_x\phi + \gamma L\phi = 0 \ \text{ at } \ x = -1.\end{cases}$$

Eq. (5) can now be solved by variable separation

$$\phi(x, t) = e^{pt}\psi(x),$$

in such a way that $\psi(x)$ satisfies the eigenvalue problem

$$\psi'' + Lc\psi' + \left[(\mu - p)L^2\right]\psi = 0, \tag{7}$$

whose solution is given by

$$\psi(x) = e^{-\alpha x}(C_1\cos Kx + C_2\sin Kx)$$

where $\alpha = \frac{Lc}{2}$ and $K^2 = L^2(\mu - p - \frac{c^2}{4})$.

It follows that the solution ϕ of our linear PDE (5) can be written as

$$\phi(x, t) = e^{pt}\psi(x) = e^{-(\alpha x - pt)}(C_1\cos Kx + C_2\sin Kx). \tag{8}$$

At this point, we impose boundary conditions and obtain the dispersion relation

$$\tan 2K = \frac{K\{(1-\gamma)[\beta L - \alpha(1-\beta)] - (1-\beta)[\gamma L - \alpha(1-\gamma)]\}}{[\beta L - \alpha(1-\beta)][\gamma L - \alpha(1-\gamma)] + K^2(1-\beta)(1-\gamma)} \tag{9}$$

which has an infinite (countable) number of roots, corresponding to the various linear instabilities (see Fig. 1). Note that $K = 0$ is not an acceptable solution. In fact, if $K = 0$, the solution (8) of the PDE would contain the sole constant C_1, and so of necessity it cannot be the solution to a second-order differential equation.

The equation for K allows us to calculate the growth/decay rate p (see Fig. 1)

$$p = \mu - \frac{K^2}{L^2} - \frac{c^2}{4}$$

and to define the steady onset μ_f to be the value of μ for which $p = 0$, i.e., the value of μ corresponding to a marginal solution, which neither grows nor decays

$$\mu_f = \frac{K^2}{L^2} + \frac{c^2}{4}.$$

3.1.2. Weakly nonlinear theory

At this point we proceed through the weakly nonlinear analysis, and first consider the nonlinear evolution PDE

$$\partial_t\Phi = \frac{c}{L}\partial_x\Phi + \frac{1}{L^2}\partial_{xx}\Phi + \Phi(\mu - \Phi) \tag{10}$$

subject to Robin boundary conditions.

The idea of weakly nonlinear theory consists in looking, close to the bifurcation point μ_f, for a simplified description of the dynamical system in terms of an amplitude equation and deducing

the approximate solutions of the PDE by imposing that the amplitude equation be steady. For Eq. (10), the solution of the PDE is expressed in the form

$$\phi(x,T) = \delta A(T) f(x) + \delta^2 B(T) g(x) + O(\delta^3) \tag{11}$$

where $B(T)g(x)$ is a second-order correction to the linear expansion. In fact, both μ and t (as well as Φ) admit an expansion in powers of δ

$$\mu = \mu_f + \delta\mu_1 + O(\delta^2) \ , \ T = \delta t.$$

At the first nonlinear order $O(\delta^2)$, the equation reads

$$B(T)\mathcal{L}g = \frac{\partial A}{\partial T} f - \mu_1 A f + A^2 f^2. \tag{12}$$

From the linear theory we know that the solution is marginal, with the linear eigenfunction satisfying $\mathcal{L}f = 0$, and therefore $\mathcal{L}$ is not invertible.

It follows, according to the Fredholm alternative theorem, that Eq. (12) has solutions only if an appropriate solvability condition is imposed.

Multiplying both sides of (12) by an unknown function f^* and integrating over the domain $x \in [-1, 1]$, we obtain (after integrating by parts twice)

$$B(T)\left\{ \int_{-1}^{1} dx g\mathcal{L}^\dagger f^* + [g' f^* - g(f^*)' + cgf^*]_{-1}^{1} \right\}$$
$$= \int_{-1}^{1} dx \left[\frac{\partial A}{\partial T} f - \mu_1 A f + A^2 f^2 \right] f^* \tag{13}$$

in which the surface terms (i.e., terms evaluated at $x = -1, 1$) $[g' f^* - g(f^*)' + cgf^*]_{-1}^{1}$ emerge from the integration by parts of the left-hand side of (12) and $\mathcal{L}^\dagger$ is the adjoint operator of $\mathcal{L}$, defined by

$$\mathcal{L}^\dagger := \frac{1}{L^2}\partial_{xx} - \frac{c}{L}\partial_x + \mu_f.$$

At this point, since we are looking for an amplitude equation for $A(T)$, we will take advantage of the fact that f^* is an arbitrary function. In fact, we will choose f^* in such a way that

$$\mathcal{L}^\dagger f^* = 0$$

with boundary conditions on f^* such that the surface terms will drop out.

As far as boundary conditions on f^* are concerned, they are obtained starting from boundary conditions on g which because of linearity are identical to those on f. With this choice of f^* the whole left-hand side of Eq. (13) drops out, with the resulting

$$\int_0^L dx \left[\frac{\partial A}{\partial T} f - \mu_1 A f + A^2 f^2 \right] f^* = 0. \tag{14}$$

In Eq. (14) we remove from the integral all quantities which do not depend on x, with the result

$$\frac{\partial A}{\partial T} = \mu_1 A - \frac{\sigma_2}{\sigma_1} A^2, \tag{15}$$

where the coefficients σ_1 and σ_2 depend on the linear eigenfunction $f(x)$ and its adjoint f^* as

$$\sigma_1 = \int_{-1}^{1} dx f f^* \ , \ \sigma_2 = \int_{-1}^{1} dx f^2 f^*.$$

This amplitude Eq. (15) presents a transcritical bifurcation at $\mu = \mu_f$, i.e., the stability of the two stationary states will be switched.

Now, in order to obtain the weakly nonlinear solution, we impose that amplitude A be steady, i.e. $\frac{dA}{dT} = 0$, so that $A = \mu_1 \frac{\sigma_1}{\sigma_2}$. On the other hand, $\mu_1 = \frac{(\mu - \mu_f)}{\delta}$, a relation which allows us to interpret parameter δ introduced above as a measure of the distance from onset μ_f. Hence

$$\phi = (\mu - \mu_f)\frac{\sigma_1}{\sigma_2} f(x) \tag{16}$$

where $f(x)$ is always the linear eigenfunction.

Now, we turn our attention to the bistable equation

$$\partial_t \Phi = \frac{c}{L}\partial_x \Phi + \frac{1}{L^2}\partial_{xx}\Phi + \Phi(\mu - \Phi^2), \tag{17}$$

with cubic rather than quadratic nonlinearity, subject to the same boundary conditions.

As far as Eq. (17) is concerned, the idea of the calculation is identical, but we will use different scales due to the symmetry of the nonlinear term:

$$t = \delta^2 T \ \text{ and } \ \mu = \mu_f + \delta^2 \mu_1 + O(\delta^3).$$

Following exactly the same procedure as in the foregoing situation, we obtain amplitude equation

$$\frac{dA}{dT} = \mu_1 A - \frac{\sigma_3}{\sigma_1} A^3 \tag{18}$$

where

$$\sigma_3 = \int_{-1}^{1} dx f^3 f^* \ \text{ and } \ \sigma_1 = \int_{-1}^{1} dx f f^*.$$

Therefore, Eq. (18) shows a supercritical pitchfork bifurcation (subcritical if $\frac{\sigma_3}{\sigma_1} < 0$). The corresponding weakly nonlinear solution is obtained in exactly the same way as it was in the transcritical case, and gives

$$\phi(x) = \sqrt{(\mu - \mu_f)\frac{\sigma_1}{\sigma_3}} f(x). \tag{19}$$

In Fig. 2, weakly nonlinear solutions (16) and (19) are compared with time-stepping for Eqs. (10) and (17). We may observe that the agreement between weakly nonlinear solution and time-stepping PDE is of order $\mu - \mu_f$.

3.1.3. Oscillatory linear theory

Thus far, we have seen that if we move away from the trivial state $\Phi = 0$, then for $\mu > \mu_f$, there correspond to every instability bifurcating steady branches which, in a neighborhood of μ_f, are of the transcritical (pitchfork) type. At this point, we want to look for oscillating solutions in the linear approximation, i.e., of the form

$$\Phi(x) = f(x)e^{i\omega t} + c.c. \ \text{ with } \ \omega \neq 0. \tag{20}$$

In other words, we want to see if it is possible to observe, as μ increases, a transition from a stable fixed point into a limit cycle, oscillating with frequency ω.

To this end, we start from the linearized equation, reduced to a self-adjoint form

$$\partial_t \hat{\Phi} = \frac{1}{L^2}\partial_{xx}\hat{\Phi} + \mu'\hat{\Phi}, \tag{21}$$

where $\mu' = \mu - \frac{c^2}{4}$.

Eq. (21) is linear. Thus we can assume that

$$\hat{\Phi}(x,t) = e^{i\omega t} g(x),$$

so that the equation for $\hat{\Phi}$ becomes

$$(i\omega - \mu')\hat{\Phi} = \frac{1}{L^2}\partial_{xx}\hat{\Phi}. \tag{22}$$

Multiplying by the complex conjugate function $\hat{\Phi}^*$ (note that in the preceding calculations we used f^* to indicate the adjoint function to f) and integrating throughout the domain, we obtain

$$(i\omega - \mu')\int_{-1}^{1} dx \hat{\Phi}\hat{\Phi}^* = \frac{1}{L^2}\int_{-1}^{1} dx \hat{\Phi}^* \partial_{xx}\hat{\Phi}. \tag{23}$$

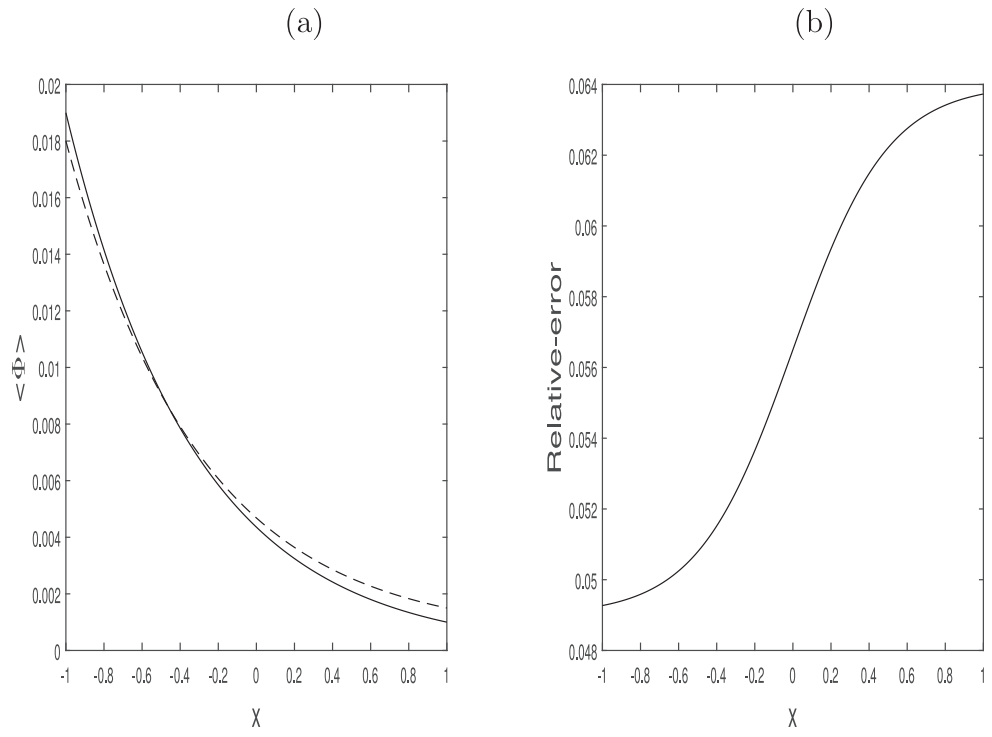

Fig. 2. (a) Time-stepping solution of Eq. (10) against weakly nonlinear solution with (b) corresponding relative error for $\mu = \mu_f + 10^{-2}$. We have assumed $L = 6$, $c = 1$, $\beta = 0.8$, $\gamma = 0.2$.

Now, if there is Hopf bifurcation from the trivial state, it will be possible to find a nonzero real number ω for which Eq. (23) is satisfied. The integral to the left is real by definition; therefore it remains to evaluate the one on the right-hand side. This is readily accomplished by integrating twice by parts, with the result that the right-hand side of Eq. (23) is real. Therefore the left-hand side must be so as well, and this is true only if $\omega = 0$.

This proves that there is no Hopf bifurcation from the trivial state $\Phi = 0$. Similarly, if we adopt transformation $\Phi \to \Phi - \mu$, we can prove that from $\Phi = \mu$ there is also no Hopf bifurcation. This is valid only if $\Phi = \mu$ is a solution, which is true solely for Neumann boundary conditions.

3.1.4. Steady-state solutions

Here, our purpose is to look at steady-state solutions of Eqs. (10) and (17), still subject to Robin boundary conditions. Therefore, we set $\partial_t \Phi = 0$ and treat the resulting ODE as a boundary value problem

$$\frac{1}{L^2}\phi'' + \frac{c}{L}\phi' + \phi(\mu - \phi) = 0 \tag{24}$$

with boundary values given by

$$\begin{cases} (1-\beta)\phi' + \beta L\phi = 0 \ \text{ at } \ x = 1 \\ (1-\gamma)\phi' + \gamma L\phi = 0 \ \text{ at } \ x = -1. \end{cases}$$

The steady-state ODE (24) can be solved using the shooting method. We rewrite the above equation as a system of two first-order ODEs,

$$\begin{cases} \phi' = \psi \\ \psi' = -Lc\psi - L^2\phi(\mu - \phi), \end{cases}$$

pick an arbitrary value of ϕ, say ϕ_0, at the left edge of the domain, so that the corresponding initial condition for the above system will be, by construction, $(\phi_0, \frac{\gamma L}{\gamma - 1}\phi_0)$.

Now, we "shoot", i.e., integrate the system up to the other boundary value, where we obtain $(\phi, \psi = \phi')$. Here we evaluate the quantity

$$\vartheta = (1-\beta)\phi' + \beta L\phi.$$

In general, for an arbitrary value ϕ_0, ϑ will not vanish, i.e., the boundary condition at the right edge of the domain will not be satisfied.

At this point we repeat the same procedure with different values of ϕ_0, until we find two values of ϕ_0, say ϕ_0^a and ϕ_0^b, for which ϑ has the opposite sign. Then, proceeding via bisection, we find the value ϕ_0 such that $\vartheta = 0$. It follows that $(\phi_0, \psi_0 = \frac{\beta L}{\beta - 1}\phi_0)$ will be the right initial condition for which both boundary values are satisfied.

The integration in space is performed by a Runge-Kutta method (always following a power law) which results in the desired accuracy.

Fig. 3 shows the shooting method applied to Eq. (24) along with its cubic variant. We observe that as the size L of the domain is increased, multiple solutions appear, though not all of them are necessarily stable.

Fig. 3b presents another interesting feature which merits comment. In fact $\vartheta(\Phi_0)$ not only oscillates, giving rise to multiple roots, but these oscillations become much more dense as they approach a limit value, say Φ_{0lim}, beyond which ϑ is not defined. This value Φ_{0lim} represents a threshold over which no steady solutions departing from Φ_0 will satisfy boundary conditions. In other words, Φ_{0lim} represents the value where the stable manifold intersects boundary conditions.

For both nonlinearities, once we fix the coefficients β and γ in the boundary conditions, Φ_{0lim} no longer depends on the size of the domain L. Furthermore, Φ_{0lim} is seen to increase remarkably at larger values of both forcing μ, and group velocity c.

At this point, let us return to the discussion of the structure of these different steady solutions. This requires a detailed analysis in phase space; we investigate the behaviour of Eq. (24), first, and thereafter extend our results to the bistable equation.

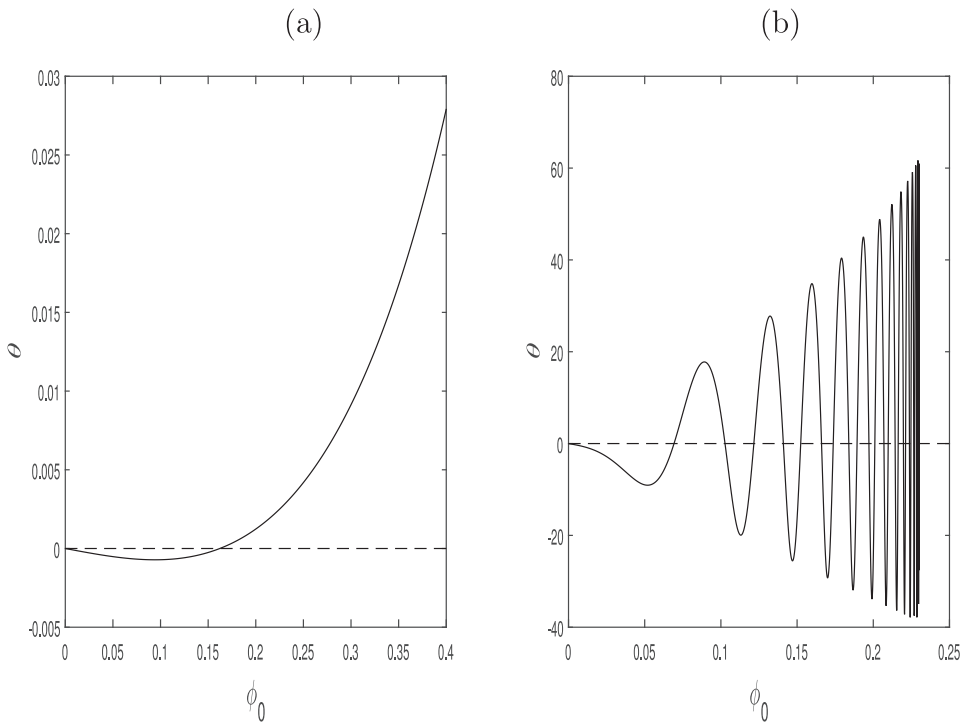

Fig. 3. (a) Shooting method applied to the equation with cubic nonlinearity for $\mu = \mu_f + 10^{-2}, L = 2,\ c = 1,\ \beta = 0.8,\ \gamma = 0.2$; (b) Shooting method applied to the equation with quadratic nonlinearity for $L = 10,\ \ c = 1,\ \ \mu = 1\ \ \beta = 0.7\ \ \gamma = \frac{\beta}{2\beta - 1}$.

Let us consider the ODE

$$\begin{cases} \Phi' = \Psi \\ \Psi' = -Lc\Psi - \mu L^2\Phi + L^2\Phi^2 \end{cases}$$

along with its fixed points, which are $(\Phi, \Psi) = (0, 0)$ and $(\Phi, \Psi) = (\mu, 0)$. For the sake of simplicity, let us maintain all other fixed parameters ($L = 10,\ \ \mu = 1$) and examine, depending on c, the qualitative behaviour of these fixed points. The linear stability analysis allows us to conclude that, if $c > 0$, the fixed point is asymptotically stable (in particular, for $0 < c < 2$ the convergence towards the fixed point will be oscillating). If $c = 0$ there are purely imaginary eigenvalues and we cannot say anything about the stability (in space) of (0,0). Similarly, we can see that (1,0) is a saddle point.

The same analysis can be performed on the ODE associated with the bistable equation, where now $(\mu,\ 0)$ is replaced by two symmetric fixed points $(\pm\sqrt{\mu}, 0)$. Stability analysis (with the same choice of parameters) provides the following results:

(i) the fixed point $\Phi = 0$ is asymptotically stable for all $c > 0$ (oscillating for $0 < c < 2$);
(ii) for all c the fixed points $\Phi = \pm\sqrt{\mu}$ have eigenvalues with opposite signs. Hence it is a saddle point.

Fig. 4, for example, shows the behaviour of steady solutions of Eq. (10) both in physical and in phase space. We observe that as parameters change (in this case c) new steady solutions can appear and are seen to emerge at small amplitude.

Now, presuming that a steady state is reached (not necessarily true, in general), we next examine the stability of these steady solutions. In fact, if we integrate the time-dependent PDE for long enough, only one of these steady solutions is selected. Here the point is that for both Eqs. (10) and (17), while solving the system of ODEs can provide (depending on initial conditions) all possible steady solutions, the integration of the time-dependent PDE detects only the stable solution.

To further our investigation, we now look at the various branches departing from the trivial state corresponding to the steady solutions.

To accomplish this, we adopt numerical continuation to study how steady solutions change as the forcing μ increases. Next, we repeat the procedure using the time-dependent PDE and compare the two. The next Fig. 5 shows the first few branches emerging from the trivial state $\phi = 0$.

Fig. 5 also plots the steady branch generated by using the time-dependent PDE. We can see that this branch follows the first steady branch departing from the onset value μ_f (which is the same for both equations because it comes from the linear theory). This proves that (at least for this choice of parameters) only the first branch is stable, while all others are not.

Still in the context of a bounded domain, our objective is to find persistent travelling waves. In order to detect time-dependent solutions it might be worth investigating the dynamics of our equation with a different set of boundary conditions. Again, focusing our analysis on the symmetry properties of our dynamical system, an interesting issue to explore might be to introduce an additional symmetry, namely, the translational, in such a way that the only symmetry-breaking is due to a violation of the reflection symmetry. We investigate the dynamics in a periodic domain.

3.2. Periodic boundary conditions

The investigation follows the pattern outlined in the preceding section, initially exploring linear theory, where we discover that the effect of translational invariance is to generate a set of instabilities corresponding to each Fourier mode considered. Thereafter, we introduce the nonlinear term and the weakly nonlinear theory, which we will discover to be very similar for both cubic and quadratic nonlinearities, with one exception, namely, Fourier mode with wave number $k = 0$ which produces different behaviours. The section will conclude by looking at the first nontrivial truncated version of our dynamical system, where the PDE is approximated

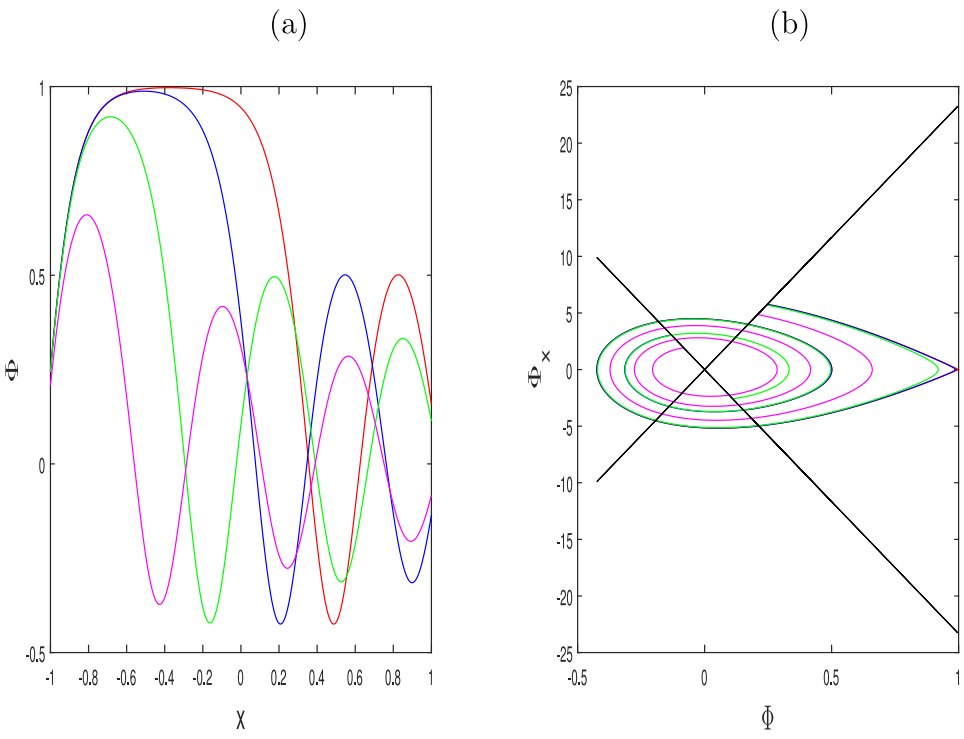

Fig. 4. (a) Steady solutions of Eq. (10) for $L = 10,\ c = 0.1,\ \beta = 0.7,\ \gamma = \frac{\beta}{2\beta-1}$ in physical space; (b) Representation in phase space of steady solutions plotted in the figure at the left (the straight line with negative and positive slope represents the boundary conditions, respectively, at $x = 1$ and $x = -1$).

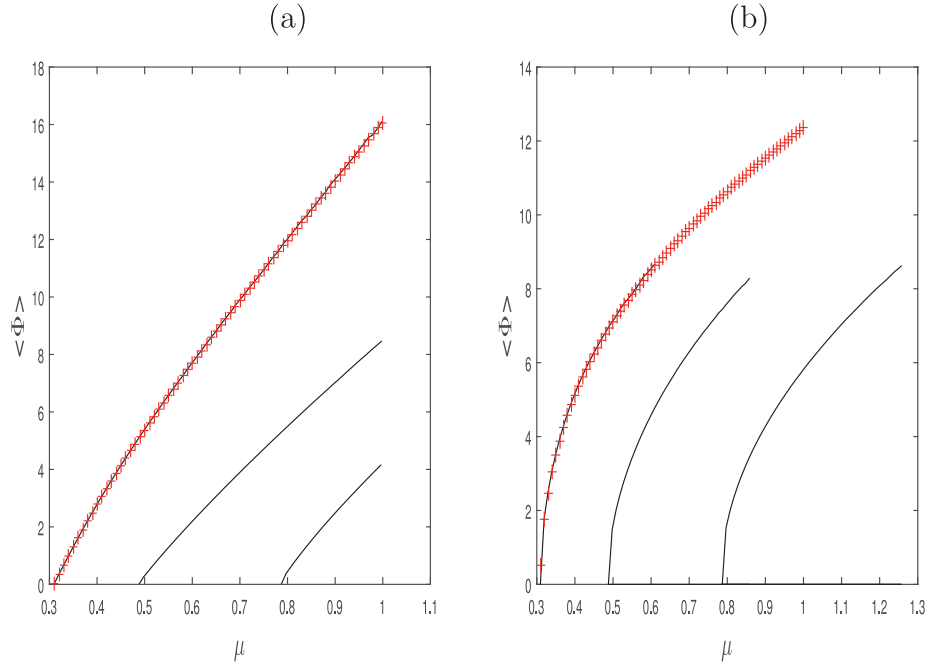

Fig. 5. Steady bifurcations of Eqs. (10) (a) and (17) (b), obtained for $L = 6,\ c = 1,\ \beta = 0.7,\ \gamma = \frac{\beta}{2\beta-1}$, compared with time-tepping PDE. In case (a), bifurcations are of the transcritical type, while in situation (b) bifurcations are of pitchfork type, as expected from the weakly nonlinear analysis.

by ODEs obtained by taking into account the evolution in time of the Fourier modes with wavenumbers up to 1.

3.2.1. Linear theory

Let us begin by setting down the nonlinear equation

$$\partial_t \Phi = \frac{1}{L^2}\partial_{xx}\Phi + \frac{c}{L}\partial_x \Phi + \Phi(\mu - \Phi^2) \tag{25}$$

with periodic boundary conditions

$$\Phi(x,t) = \Phi(x + 2\pi, t).$$

We drop the nonlinear term and separate variables, $\Phi(x,t) = T(t)F(x)$ in order to obtain the eigenvalue problem

$$\begin{cases} T' = \sigma T \\ \frac{1}{L^2}F'' + \frac{c}{L}F' + (\mu - \sigma)F = 0 \end{cases}$$

where in general $\sigma \in \mathbb{C}$. At this point, if we assume F to be spatially periodic on $[0, 2\pi]$, of the form $F(x) = e^{ikx}$, with $k \in \mathbb{Z}$, we obtain dispersion relation

$$\sigma = \left(\mu - \frac{k^2}{L^2}\right) + i\left(\frac{ck}{L}\right). \tag{26}$$

It follows that the analytical solution Φ may be expressed as

$$\Phi = \exp(\sigma t)\exp(ikx) = \exp\left[\left(\mu - \frac{k^2}{L^2}\right)t\right]\exp\left[ik\left(x + \frac{c}{L}t\right)\right] \tag{27}$$

where the first exponential represents the growth/decay rate, the second a travelling wave. Here, therefore, emerges the first crucial difference from the asymmetric conditions: the location of instabilities and growth rate do not depend on group velocity c, which produces merely a shift of our solutions to the left or right depending on the sign of c. This is a consequence of the translational invariance ($x \to x + L$) of periodic domains. In addition, if we look at Eq. (26) it is evident that, for $c \neq 0$, as $\mu = \frac{k^2}{L^2}$ the real part of the eigenvalue vanishes, but not the imaginary one (as long as $k \neq 0$). This means that, corresponding to each wavenumber k, there are branches emerging from the trivial state via Hopf bifurcation, thus giving rise to time-dependent solutions.

3.2.2. Weakly nonlinear theory

The exploration of the weakly nonlinear theory resembles the one already seen for the case of asymmetric boundaries, but some differences emerge as the discussion goes on. We can take advantage of the translational invariance and set $c = 0$, which corresponds to performing the transformation $\tilde{x} = x + \frac{c}{L}t$, and study the problem in the moving frame. We begin by investigating the bistable equation, and then extend our results to the problem with quadratic nonlinearity. Again, we introduce various time scales $T_0 = t$, $T_1 = \delta t, T_2 = \delta^2 t$ and expand both our solution Φ, and the forcing term μ, in powers of a small parameter δ:

$$\Phi = \delta\Phi_1 + \delta^2\Phi_2 + \delta^3\Phi_3 + O(\delta^4), \quad \text{with} \quad \Phi_1 \neq 0$$

$$\mu = \mu_0 + \delta\mu_1 + \delta^2\mu_2 + O(\delta^3).$$

If we plug the entire expansion into Eq. (25), at the leading order $O(\delta)$ we obtain:

$$\frac{\partial\Phi_1}{\partial T_0} = \mathcal{L}\Phi_1 \tag{28}$$

where $\mathcal{L}$ is the linear differential operator defined by $\mathcal{L} := \frac{1}{L^2}\partial_{xx} + \mu_0$.

If we define in our functional space an inner product

$$\langle f, g\rangle := \int_0^{2\pi} dx f g$$

we can also define the adjoint of $\mathcal{L}$, $\mathcal{L}^\dagger$, from the relation

$$\langle \mathcal{L}f, g\rangle = \langle f, \mathcal{L}^\dagger g\rangle.$$

If group velocity $c = 0$, $\mathcal{L}$ is self-adjoint.

Now, the solution of Eq. (28) corresponding to $\mu = \mu_0$ is marginal; hence its growth rate vanishes, which means that the time scale T_0 is not relevant and can be ignored.

Hence, the solution Φ_1 of the linearized problem takes the form $A(T_1, T_2)f(x)$, where A is in general a complex amplitude, $f(x)$ is the linear eigenfunction, and Φ_1 satisfies $\mathcal{L}\Phi_1 = 0$. This equation has two solutions, $\Phi_1 = 0$, which is not acceptable because of our ansatz; and $\Phi_1 = Ae^{ikx} + \bar{A}e^{-ikx}$, under the assumption of $k \neq 0$, where amplitude A can in principle depend on both time scales T_1 and T_2. At the first nonlinear order $O(\delta^2)$, we obtain

$$\frac{\partial\Phi_1}{\partial T_1} = \mathcal{L}\Phi_2 + \mu_1\Phi_1. \tag{29}$$

The calculation at the leading order has shown us that $\mathcal{L}\Phi_1 = 0$ and so $\mathcal{L}$ is not invertible. Therefore, we impose the solvability condition simply by requiring the equation to be orthogonal to all eigenfunctions of the adjoint problem

$$\left\langle \frac{\partial\Phi_1}{\partial T_1}, e^{-ikx}\right\rangle = \left\langle \mathcal{L}\Phi_2, e^{-ikx}\right\rangle + \mu_1\left\langle \Phi_1, e^{-ikx}\right\rangle. \tag{30}$$

After evaluating the inner products, we remain with

$$\frac{\partial\Phi_1}{\partial T_1} = \mu_1\Phi_1.$$

The previous equation is still linear; thus its solutions must grow exponentially. Therefore, we set $\mu_1 = 0$ in such a way that time scale T_1 also becomes irrelevant. As a consequence, amplitude A can now be a function of the only remaining time scale T_2.

At order $O(\delta^3)$ the equation to solve is

$$\frac{\partial\Phi_1}{\partial T_2} = \mathcal{L}\Phi_3 + \mu_2\Phi_1 - \Phi_1^3. \tag{31}$$

We impose once more the solvability condition, and find

$$\frac{\partial A}{\partial T_2} = \mu_2 A - 3|A|^2 A \tag{32}$$

which represents the normal form of a pitchfork bifurcation.

Note that we have developed the calculation only for the first term of Φ because for the complex conjugate it would be identical. At this point, we require amplitude A to be steady and find the weakly nonlinear solution

$$\Phi = \delta\Phi_1 = \delta\sqrt{\frac{\mu_2}{3}}\left(e^{i(kx+\phi)} + c.c\right)$$
$$= 2\sqrt{\frac{\mu - \mu_0}{3}}\cos(kx + \phi) + O(\delta^3). \tag{33}$$

If $k = 0$, there is only one linearly independent eigenfunction: $\psi = 1$. In this case, a calculation very similar to the one above leads to the solution $\Phi = \sqrt{\mu}$. Clearly, if $\sqrt{\mu}$ is a solution, so is $-\sqrt{\mu}$. We note that in the case of $k = 0$ the weakly nonlinear solution is actually the exact solution of the fully nonlinear problem.

Similarly to the case of asymmetric boundaries, Fig. 6 shows the solution of the time-stepping PDE plotted against the weakly nonlinear solution in the case of wavenumber $k = 0$, first, and then for $k \neq 0$. If we had a reflection symmetry break due to the presence of a non-zero group velocity $c \neq 0$, the calculation would have been identical (with the same result), except for a new definition of the differential operator $\mathcal{L}$

$$\mathcal{L} := \frac{c}{L}\partial_x + \frac{1}{L^2}\partial_{xx} + \mu_0 - \partial_{T_0}$$

to prevent amplitude A from evolving on the fast time scale.

As far as the problem with quadratic nonlinearity is concerned, we can repeat the identical calculation outlined above, with surprising results. If $k = 0$ we obtain a transcritical bifurcation, just as in the case of Robin boundary conditions, where the weakly nonlinear solution, $\Phi = \mu$, would actually be the solution to the fully nonlinear problem. In contrast, if $k \neq 0$ the analytical calculation leads to a bifurcation of pitchfork type, just as in the bistable case, with the weakly nonlinear solution given by

$$\Phi = 2\left[\left(\frac{3k^2}{10L^2}\right)\sqrt{\mu - \frac{k^2}{L^2}}\right]\cos(kx + \phi).$$

This last result can be explained as follows. The translation by a distance d acts on the solution Φ as $\Phi(x, t) \to \Phi(x - d, t)$. Therefore, the corresponding action on the amplitude $A(t)$ is $A(t)e^{-ikd}$. This means that if $k \neq 0$ the amplitude equation for $A(t)$ must be equivariant with respect to phase shifts. Therefore, in the case of

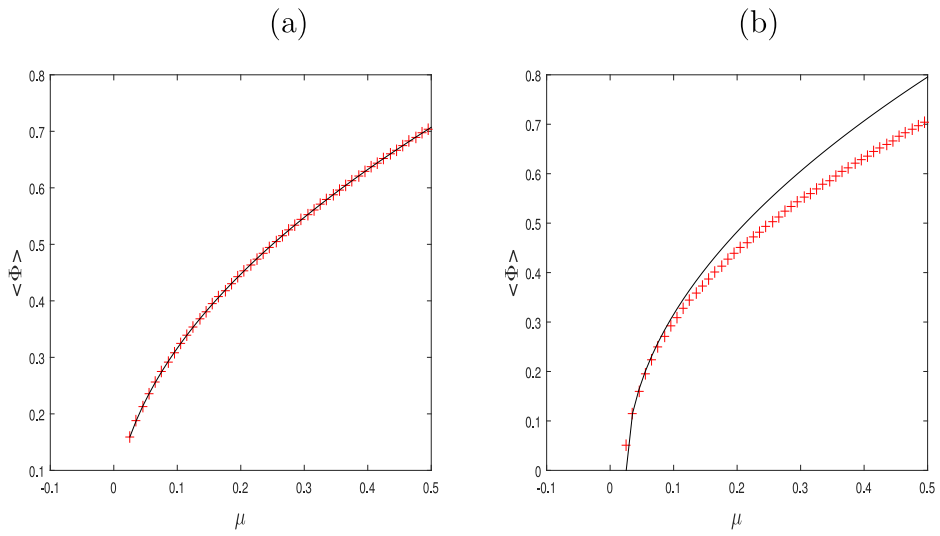

Fig. 6. Pitchfork branches (continuous line) deduced from the bistable equation for $L = 2\pi$, $c = 0$, compared with time-stepping Eq. (25) (crosses line) in the case of (a) $k = 0$ and (b) $k \neq 0$.

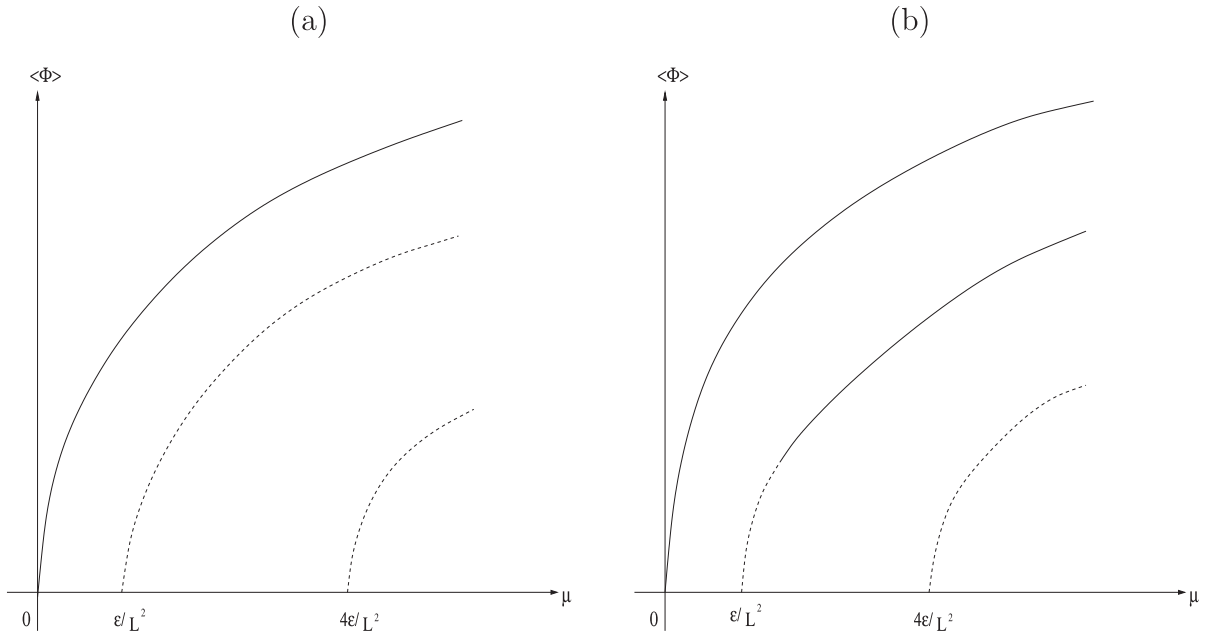

Fig. 7. Schematic bifurcation diagram for the PDE (25) obtained for (a) $L = 5$ and (b) $L = 12$.

quadratic nonlinearity, if we had a transcritical normal form, it would result in

$$\dot{A} = \mu A - A^2 e^{ikd}.$$

If $k = 0$, then the translation symmetry does nothing. In this case, the quadratic nonlinearity allows no change-of-sign symmetry and therefore we have a transcritical normal form, whereas, by contrast, cubic nonlinearity does allow change-of-sign symmetry, and hence a pitchfork normal form. For all other values of k the term $A^2 e^{ikd}$ must vanish, the reason for which being if $k \neq 0$ we end up with a pitchfork bifurcation, regardless of the nonlinearity.

As to stability, after considering solutions corresponding to the steady branch ($k = 0$) and to the first travelling wave ($k = 1$), we have added a perturbation containing different wavenumbers and observed the evolution in time of the perturbation. We limit our discussion to the bistable case, because we obtain similar results in the case of quadratic nonlinearity. For both steady branches (transcritical and pitchfork) the perturbations quickly decay to zero, thus confirming their stability. In contrast, the travelling waves exhibit a different dynamic: if the size of the domain L is small they are unstable to the steady branches throughout, while as L is increased, they appear unstable initially, and then gain stability.

Fig. 7 shows a schematic bifurcation diagram corresponding to different lengths of the domain. The study of a reduced model will help us understand this in deeper detail.

3.2.3. Truncated model

At this juncture, in order to further investigate the dynamics of all possible solutions obtained by varying the forcing μ, we take advantage of our solution Φ being spatially periodic and consider its truncated expansion in Fourier series, ignoring all terms with $k > 1$, so that the truncated solution will look like

$$\Phi = a_0 + a_1 \cos x + b_1 \sin x. \tag{34}$$

Substituting (34) into our main Eq. (25) and comparing coefficients, we obtain a system of three coupled ODEs, a system which

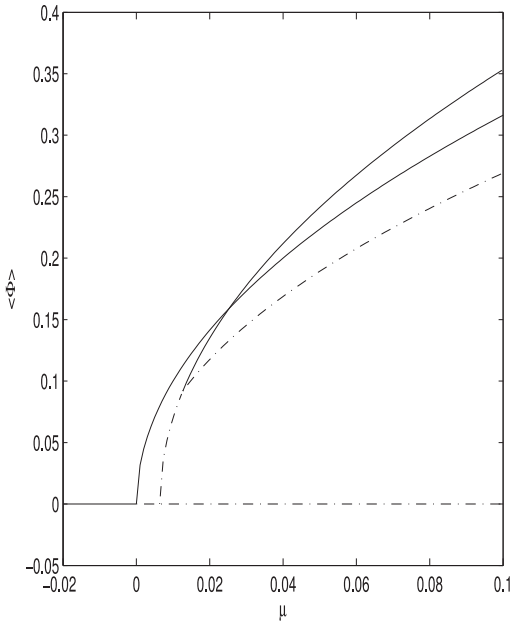

Fig. 8. Bifurcation diagram for the ODE (35) obtained for $L = 12$, $c = 3$.

describes the evolution in time of Fourier coefficients a_0, a_1 and b_1

$$\begin{cases} \dot{a}_0 = \mu a_0 - a_0^3 - \frac{3}{2}a_0(a_1^2 + b_1^2) \\ \dot{a}_1 = \frac{c}{L}b_1 + \left(\mu - \frac{1}{L^2}\right)a_1 - 3a_0^2 a_1 - \frac{3}{4}a_1(a_1^2 + b_1^2) \\ \dot{b}_1 = -\frac{c}{L}a_1 + \left(\mu - \frac{1}{L^2}\right)b_1 - 3a_0^2 b_1 - \frac{3}{4}b_1(a_1^2 + b_1^2). \end{cases} \tag{35}$$

It is readily seen that if $\mu \leq 0$, the only fixed point is (0,0,0) which is stable, while as μ becomes positive, (0,0,0) loses stability via a supercritical pitchfork bifurcation, and two other symmetric, stable, fixed points are found, namely, $(\pm\sqrt{\mu}, 0, 0)$. In particular, the trivial state has one real eigenvalue, μ, and a pair of complex conjugate eigenvalues, whose real part vanishes as $\mu = \frac{1}{L^2}$, thus giving rise to a Hopf bifurcation. Aiming to investigate the stability of the resulting periodic orbit, we switch onto polar coordinates (which maps the periodic orbit onto a fixed point) and perform linear stability analysis, with the result that the unstable periodic orbit, emerging from the trivial state, gains stability at $\mu = \frac{2}{L^2}$ through a subcritical pitchfork bifurcation, where two unstable branches are generated. Fig. 8 illustrates this. In particular, in this case we have only one eigenvalue with a positive real part which changes sign, thus ruling out the occurrence of a secondary Hopf bifurcation, and so we are left with a stable travelling wave as it was for the PDE.

We might note, in passing, that our use of a truncated model could well result in the loss of certain dynamical features impossible to characterize or estimate without further, more elaborate study which we would definitely encourage. Our goal herein, by contrast, has been to demonstrate that even the lowest-order nontrivial expansion captures the main qualitative features of the corresponding infinite-dimensional dynamical system, a result which our employment of a truncated model has allowed us to achieve.

4. Discussion and conclusions

This study has allowed us to deepen our knowledge of our one-dimensional reaction-diffusion system, by focusing on the simplest possible equation containing both a throughflow as well as a nonlinear term describing, for example, the particular chemical reaction or biological process one might eventually be investigating in theoretical or experimental research.

Our objective has been to examine this problem from the perspective of nonlinear dynamics, by investigating, within a bounded domain, the effect produced first by the absence, and then by the presence, of two particular symmetries: reflection and translation.

Three main ingredients have been considered: the particular choice of boundary conditions, the presence of a throughflow, and a uniform forcing which drives the system outside of equilibrium.

We have seen that with Robin boundaries there is no Hopf bifurcation from the trivial state, and that only steady states are detected after a transient. The corresponding normal forms in the weakly nonlinear regime are, respectively, of transcritical and pitchfork type for quadratic and cubic nonlinearities. With periodic boundaries, by contrast, there are travelling waves emerging from the trivial state via Hopf bifurcation corresponding to each wavenumber k, which are seen to restabilize at increased driving parameter and length of the domain. As to the normal forms obtained in the weakly nonlinear regime, for wavenumber $k = 0$ we obtain transcritical and pitchfork bifurcations just as with Robin boundaries. By contrast, for $k \neq 0$, the symmetry of the problem imposes a cubic normal form for both nonlinearities.

The introductory section of the present paper describes the work of such investigators as Taylor [27] and Beck [35] who conducted their work assuming a domain long enough that the presumption of an infinite domain was valid. The model we have developed herein would improve on this. Our model takes into account the effect of finite-distance boundaries, as a real experiment or theoretical model would require. In such a case, travelling waves cannot be reflected from boundaries. As a consequence, in a convective unstable regime, travelling waves would be expected to decay while, as the threshold of absolute instability is exceeded, waves can be maintained against dissipation at the boundaries.

Our mathematical description extends such investigators' models to the case of Robin boundary conditions, those which in fact represent the general form of insulating boundaries, namely, where the sum of convective and diffusive fluxes at the boundaries is zero.

The possible implications of taking finite-distance boundaries into account in this way are manifold: Our work might permit, for example, a more realistic theoretical description of the experiments of Taylor. We expect that experiments would confirm that when the domain is small enough, travelling waves would exist just for a transient, thus leaving us with a steady pattern. In addition we would expect that the same experiments performed in systems with periodic geometry would lead, above the absolute instability threshold, to persistent travelling waves recirculating within the domain.

Our work seeks to present a theoretical platform which would allow a much more realistic description of the problem and would aid in making the conduct and conclusions of all such investigations more precise and more complete. In addition, our work can turn out relevant in continuing the pattern established by the works of Beck and Cain [15,35]. In fact, the results obtained in the case of Robin boundaries would be in line with the findings of Cain, where the action potential can propagate more easily away from an absorbing boundary. We would expect, then, in a finite-length domain, action potential to be present at least in the central region of the domain, if the domain is long enough. This would resemble what happens in the propagation of the electric signal from the SA to the AV node, where, in the absence of an additional stimulus, there would be no wave propagation. By contrast, in the case of periodic boundaries, we believe that even a one-dimensional setting like ours would provide extremely useful information in terms of the stability of reentrant spiral waves, waves

which would, as long as in a dynamic regime above the threshold of absolute instability, exist independently of the stimulation.

The author is grateful to Angelo Di Garbo and Mario D'Acunto for many helpful discussions, and to the anonymous referees for all the invaluable comments, that contributed dramatically to improve this paper.

Declaration of Competing Interest

None.

References

[1] Cross MC, Hohenberg P. Pattern formation outside of equilibrium. Rev Mod Phys 1992;65:851–1112.
[2] Epstein IR, Golubitsky M. Symmetric patterns in linear arrays of coupled cells. Chaos 1993;3:1–5.
[3] Busse FH, Müller SC. Evolution of spontaneous structures in dissipative continuous systems. Berlin Heidelberg: Springer-Verlag; 1998.
[4] Dab D, Lawniczac A, Boon JP, Kapral R. Cellular automaton model for reactive systems. Phys Rev Lett 1990;64:2462–5.
[5] Ipsen M, Hynne F, Sorensen PG. Amplitude equations and chemical reaction-diffusion systems. Int J Bifurcation Chaos 1997;7:1539–54.
[6] Dee G, Langer JS. Propagating pattern selection. Phys Rev Lett 1983;50:383–6.
[7] Glass L, Sun J. Periodic forcing of a limit cycle oscillator: fixed points, arnold tongues, and the global organization of bifurcations. Phys Rev E 1994;50:5077–84.
[8] Thompson BW, Novak J, Wilson MCT, Britton MM, Taylor AF. Inward propagating chemical waves in taylor vortices. Phys Rev E 2010;81(4). 047101–4
[9] Deneke VE, Di Talia S. Chemical waves in cell and developmental biology. J Cell Biol 2018;217(4):1193–204.
[10] Faye G. Existence and stability of travelling pulses in a neural field equation with synaptic depression. SIAM J Appl Dyn Syst 2013;12(4):2032–67.
[11] Holzer M, Doelman A, Kaper TJ. Existence and stability of travelling pulses in a reaction-diffusion-mechanics system. SIAM J Nonlinear Sci 2013;23:129–77.
[12] Rioux M, Bourgault Y. A predictive method allowing the use of a single ionic model in numerical cardiac electrophysiology. ESAIM 2013;47:987–1016.
[13] Tsai JC. Do calcium buffers always slow down the propagation of calcium waves? SIAM J Math Biol 2013;67(6):1587–632.
[14] Rasheed SM, Omar F. A comparison between finite difference and asymptotic methods for solving a reaction-diffusion model in ecology. Int J Math Comp Meth 2016;1:29–222.
[15] Cain JW, Schaeffer DG. Shortening of cardiac action potential duration near an insulating boudary. Math Med Biol 2008;25:21–36.
[16] Cantrell RS, Cosner C, Yu X. Dynamics of populations with individual variation in dispersal on bounded domains. J Biol Dyn 2018;12(1):288–317.
[17] Kondo S, Miura T. Reaction-diffusion model as a framework for understanding biological pattern formation. Science 2010;329(5999):1616–20.
[18] Britton MM. MRI of chemical reactions and processes. Prog Nucl Magn Reson Spectrosc 2017;101:51–70.
[19] Ramirez SA, Raghavachari S, Lew DJ. Dendritic spine geometry can localize GTPase signaling in neurons. Mol Biol Cell 2015;26:4171–81.
[20] Abshagen J, Lopez JM, Marques F, Pfister G. Symmetry breaking via global bifurcations of modulated rotating waves in hydrodynamics. Phys Rev Lett 2005;94:74501–4.
[21] Barkley D. Symmetry breaking in reaction-diffusion systems. Scholarpedia 2008.
[22] Kolmogorov AN, Piskunov NS, Petrowski IG. Etude de la diffusion avec croissance de la quantite de la matiere et son application a un probleme biologique. Moscov Univ Math Bull 1937;1:1–25.
[23] Ecke RE, Zhong F, Knobloch E. Hopf bifurcation with broken reflection symmetry in rotating rayleigh-benard convection. Europhys Lett 1992;19:177–82.
[24] Van Saarloos W. Front propagation into unstable states: marginal as a dynamical mechanism for velocity selection. Phys Rev A 1988;37:211–29.
[25] Van Saarloos W. Front propagation into unstable states. Phys Rep 2003;386:29–222.
[26] Kuramoto Y. Chemical oscillations, waves and turbulence. Berlin: Springer-Verlag; 1984.
[27] Taylor A, Britton MM. Magnetic resonance imaging of chemical waves in porous media. Chaos 2006;16:1.
[28] Mitchell CC, Schaeffer DG. A two-current model for the dynamics of cardiac membrane. Bull Math Biol 2003;65:767–93.
[29] Karma A. Spiral breakup in model equations of action potential propagation in cardiac tissue. Phys Rev Lett 1993;71(7):1103–6.
[30] Qintao G, Tielin L, Chang L, Tianshi L. Synchronization for a class of generalized neural networks with interval time-varying delays and reaction-diffusion terms. Nonlinear Anal 2016;21(3):379–99.
[31] Stovold JH, O'Keefe SEM. Reaction-diffusion chemistry implementation of associative memory neural network. Int J Parallel Emergent Distrib Syst 2016;32(1):74–94.
[32] Ermentrout GB. Neural networks as spatio-temporal pattern-forming systems. Rep Prog Phys 1998;61:335–430.
[33] Dahlem MA, Müller SC. Reaction-diffusion waves in neuronal tissue and the window of cortical excitability. Ann Phys 2004;13(7):442–9.
[34] Alonso S, Bär M, Panfilov AV. Negative tension of scroll wave filaments and turbulence in three-dimensional excitable media and application in cardiac dynamics. Bull Math Biol 2013;75(8):1351–76.
[35] Beck M, Jones CKRT, Shaeffer D, Wechselberger M. Electrical waves in a one-dimensional model of cardiac tissue. SIAM J Appl Dyn Syst 2008;7(4):1558–81.
[36] Fitzhugh R. Mathematical models of threshold phenomena in the nerve membrane. Bull Math Biophys 1955;17:257–78.
[37] Fitzhugh R. Impulses and physiological states in theoretical models of nerve membrane. Biophys J 1961;1:445–66.
[38] Nagumo J, Arimoto S, Yoshizawa S. An active pulse transmission line simulating nerve axon. Proc IRE 1962;50:2061–70.
[39] Katz AM. Physiology of the heart. Philadelphia: Lippincot Williams Wilkins; 2011.
[40] Nobile F, Vergara C. An effective fluid-structure interaction formulation for vascular dynamics by generalized robin conditions. SIAM J Sci Comput 2008;30(2):731–63.
[41] Hassan SA, Zanette DH, Wio HS. Stationary states in a reaction-diffusion system with albedo boundary conditions. J Phys A 1994;27(15):5129–34.
[42] Wio HS, Izus G, Ramirez O, Deza R, Borzi C. Pattern formation in an activator-inhibitor model: effect of albedo boundary conditions on a finite geometry. J Phys A 1993;26:4281–6.
[43] Rovinsky AB, Menzinger M. Chemical instability induced by a differential flow. Phys Rev Lett 1992;69(8):1193–7.
[44] Ponce Dawson S, Lawniczak A, Kapral R. Interaction of turing and flow-induced chemical instabilities. J Chem Phys 1994;100:5211–18.
[45] Turing AM. Chemical instability induced by a differential flow. Phil Trans Roy Soc London B 1952;237:37–72.